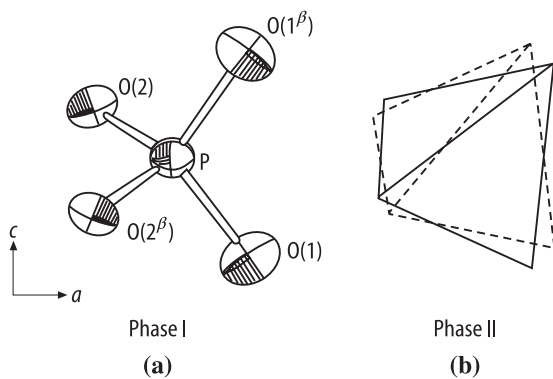
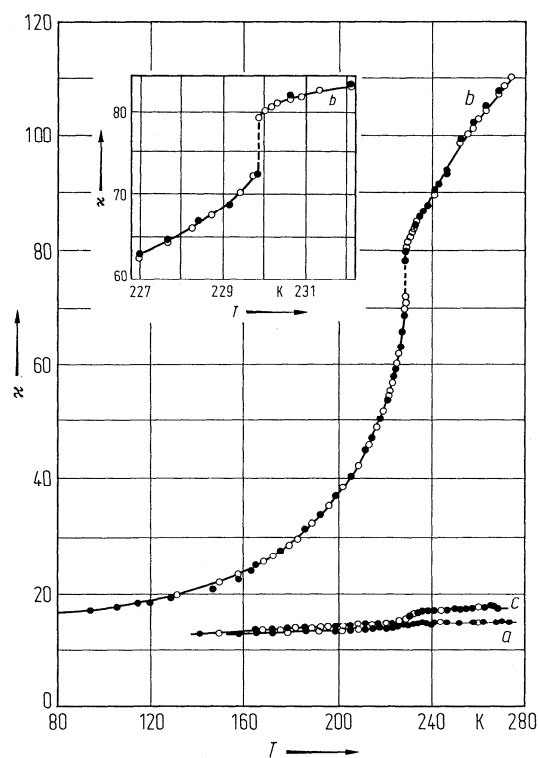


**Fig. 33A-4-001.**  $\text{TiH}_2\text{PO}_4$  (TDP). Structure at RT [79Odd]. Anisotropic temperature parameter of each atom is illustrated by ellipsoid.



**Fig. 33A-4-002.**  $\text{TiH}_2\text{PO}_4$  (TDP). Structure of  $\text{PO}_4$  tetrahedron [94Mat]. (a)  $T = 373$  K. Anisotropic temperature parameters are illustrated. (b) Two structurally equivalent orientations in phase II.



**Fig. 33A-4-003.**  $\text{TiH}_2\text{PO}_4$  (TDP).  $\kappa$  along  $a$ ,  $b$ ,  $c$  axes vs.  $T$  [77Mat].  $f = 1$  kHz. Insert:  $\kappa_b$  in the vicinity of  $\Theta_{\text{III-II}}$ .

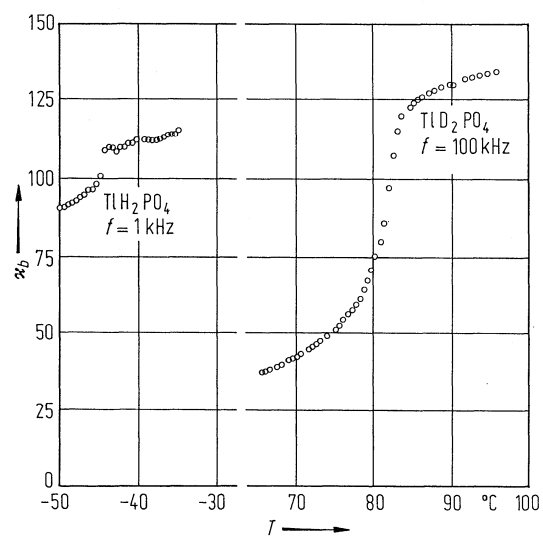


**Fig. 33A-4-004.**  $\text{TiH}_2\text{PO}_4$  (TDP),  $\text{TiD}_2\text{PO}_4$  (DTDP).  $\kappa_b$  vs.  $T$  [80Yas2].

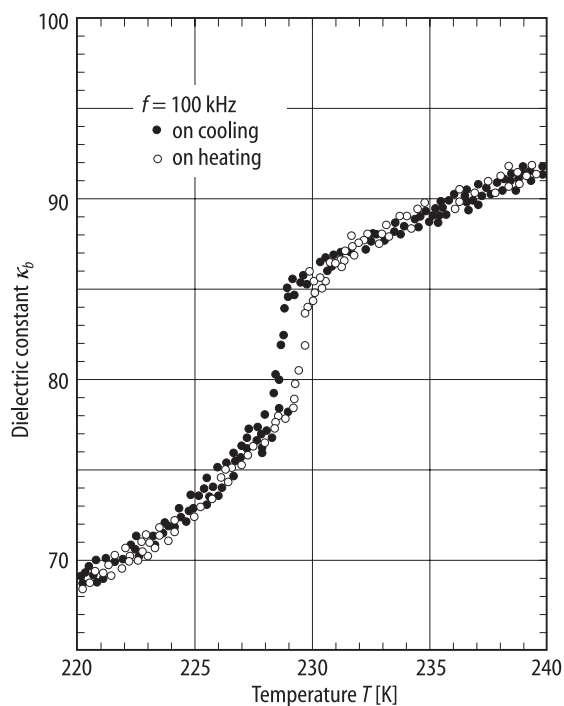


**Fig. 33A-4-005.**  $\text{TlH}_2\text{PO}_4$  (TDP).  $\kappa_b$  vs.  $T$  in the vicinity of  $\Theta_{\text{II-III}}$  [94Par].

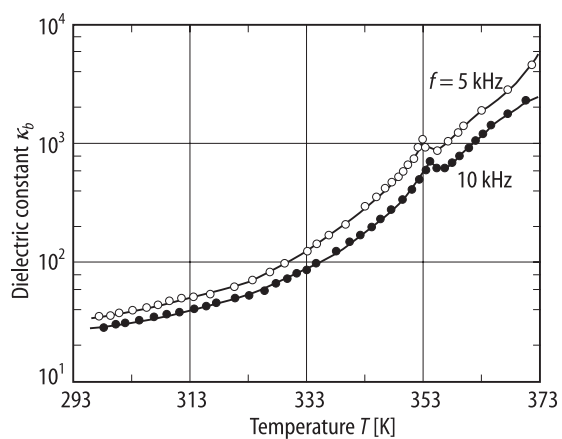


**Fig. 33A-4-006.**  $\text{TlD}_2\text{PO}_4$  (DTDP).  $\kappa_b$  vs.  $T$  [87Nar]. Parameter:  $f$ . Deuteration rate  $> 0.97$ .

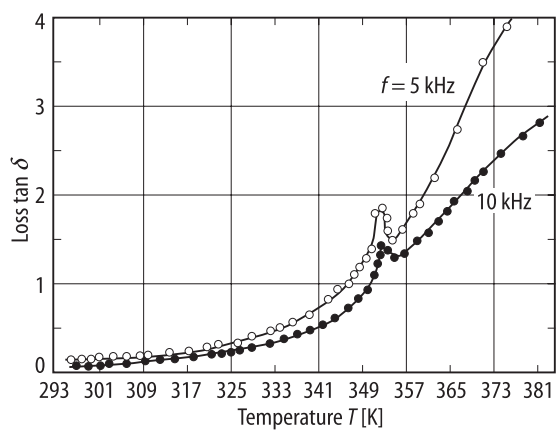


**Fig. 33A-4-007.**  $\text{TlD}_2\text{PO}_4$  (DTDP).  $\tan \delta$  vs.  $T$  [87Nar]. Parameter:  $f$ . Deuteration rate  $> 0.97$ .

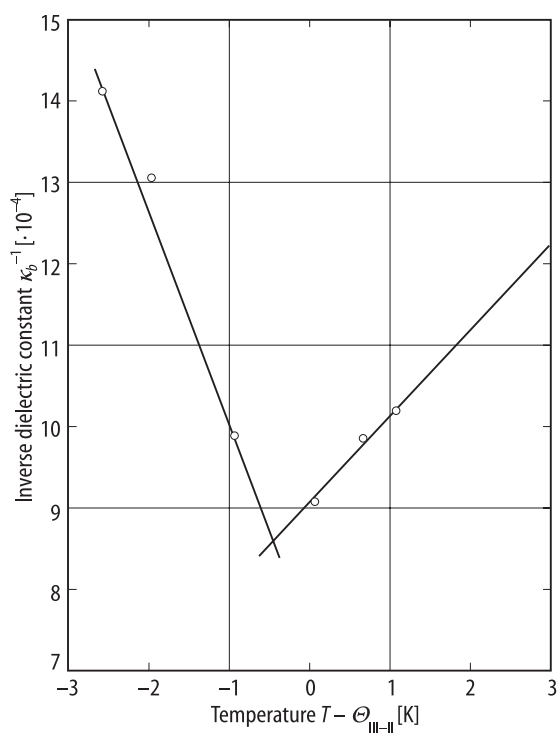


**Fig. 33A-4-008.**  $\text{TlD}_2\text{PO}_4$  (DTDP).  $1/\kappa_b$  vs.  $T - \Theta_{\text{III-II}}$  [87Nar]. Deuteration rate  $> 0.97$ .

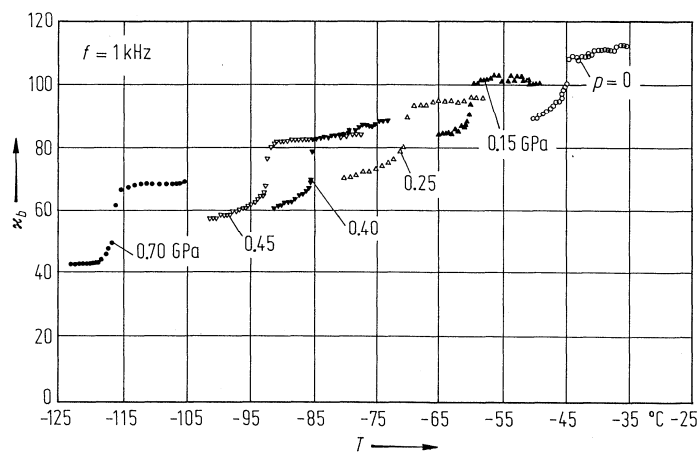


Fig. 33A-4-009.  $\text{TlH}_2\text{PO}_4$  (TDP).  $\kappa_b$  vs.  $T$  [80Yas1]. Parameter:  $p$ .

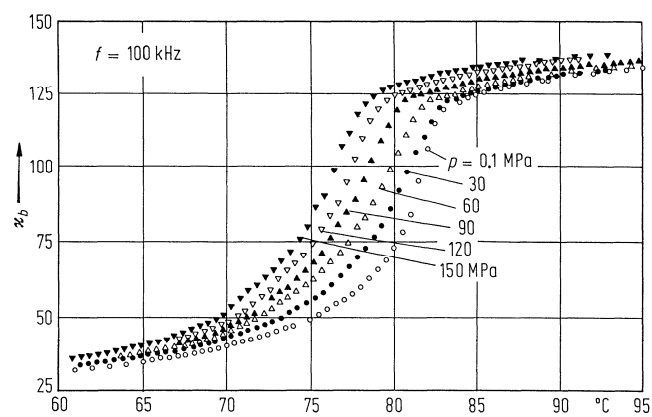


Fig. 33A-4-010.  $\text{TlD}_2\text{PO}_4$  (DTDP).  $\kappa_b$  vs.  $T$  [80Yas1]. Parameter:  $p$ .

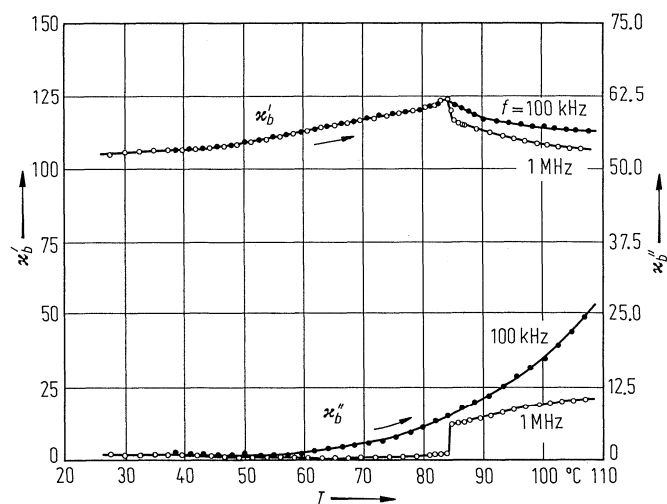
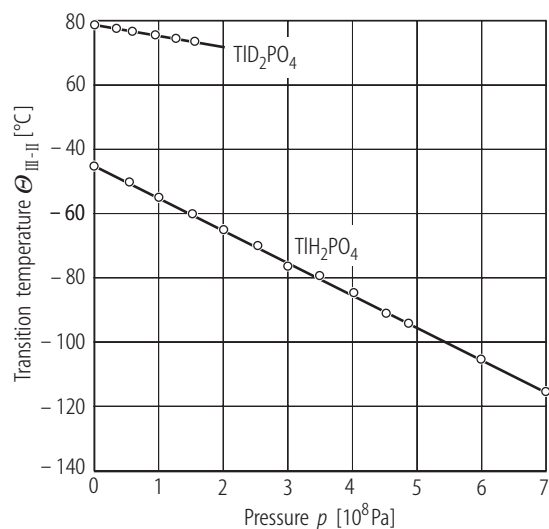
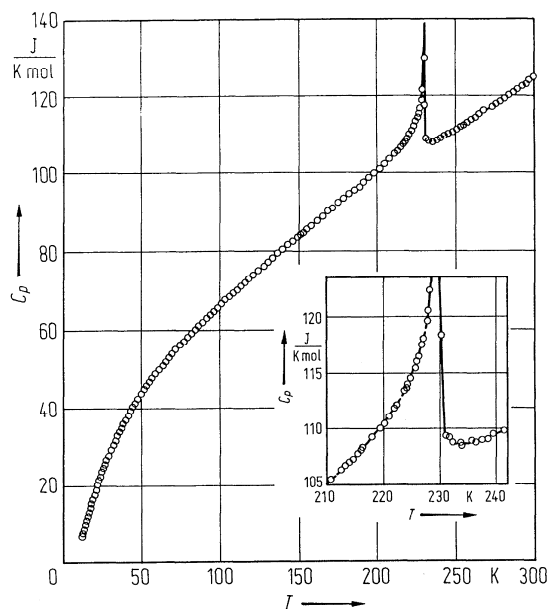


Fig. 33A-4-011.  $\text{TlH}_2\text{PO}_4$  (TDP).  $\kappa'_b$ ,  $\kappa''_b$  vs.  $T$  [84Yos]. Parameter:  $f$ .



**Fig. 33A-4-012.**  $\text{TIH}_2\text{PO}_4$  (TDP),  $\text{TID}_2\text{PO}_4$  (DTDP).  $\Theta_{\text{III-II}}$  vs.  $p$  [79Yas].



**Fig. 33A-4-013.**  $\text{TIH}_2\text{PO}_4$  (TDP).  $C_p$  vs.  $T$  [77Mat].  $C_p$ : molar heat capacity. The insert shows the behavior in the vicinity of  $\Theta_{\text{III-II}}$ .

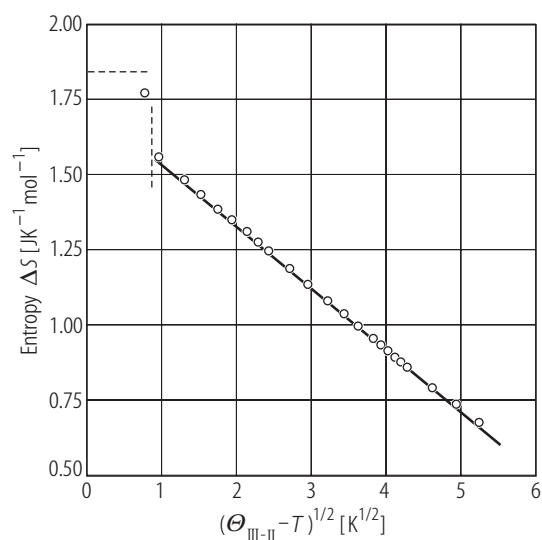


**Fig. 33A-4-014.** TIH<sub>2</sub>PO<sub>4</sub> (TDP).  $\Delta S$  vs.  $(\Theta_{\text{III-II}} - T)^{1/2}$  [77Mat].  $\Delta S$ : anomalous entropy. The horizontal broken line indicates the entropy of phase II. The vertical broken line corresponds to the temperature of the first order transition.

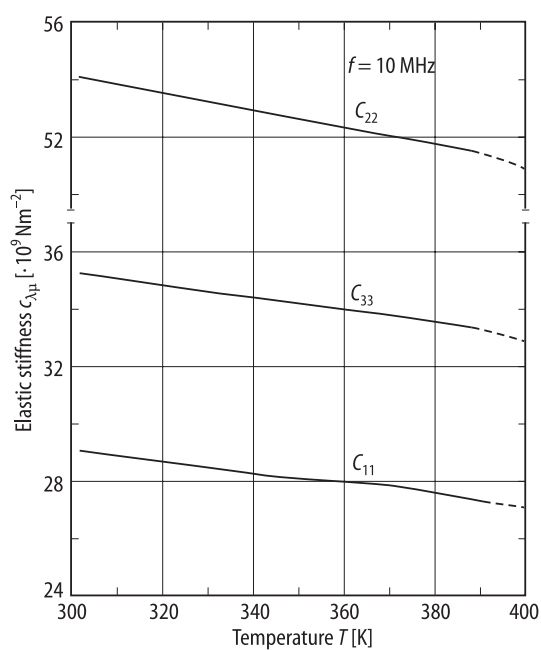
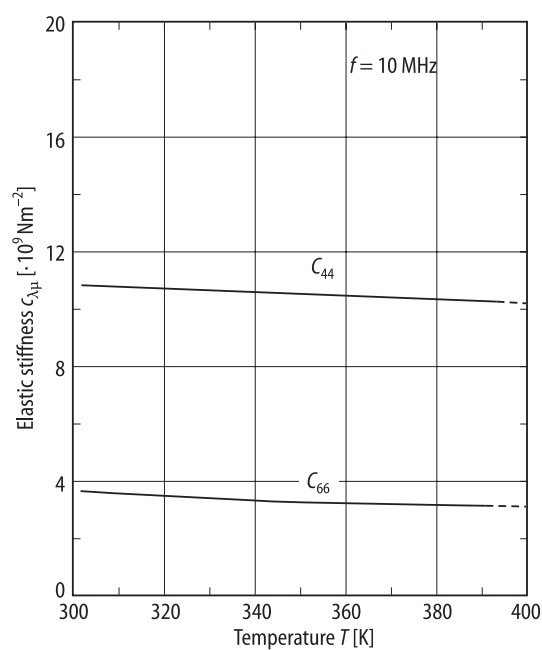


**Fig. 33A-4-015.** TIH<sub>2</sub>PO<sub>4</sub> (TDP).  $c_{\lambda\mu}$  vs.  $T$  [91Han].

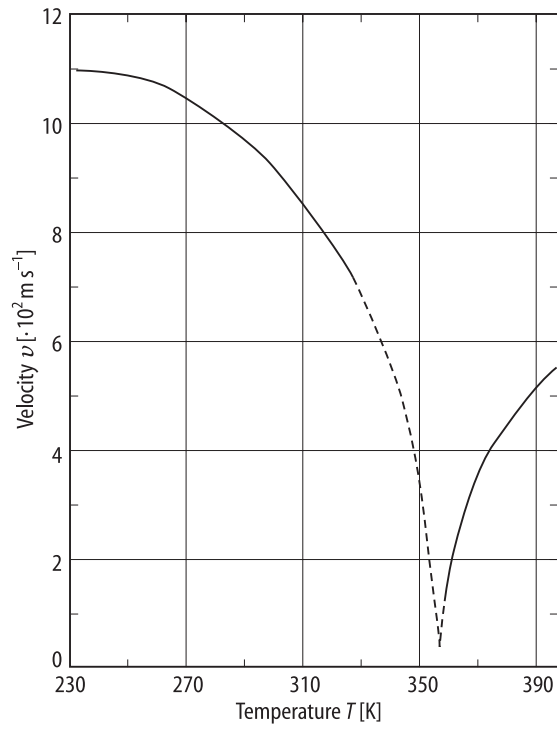


**Fig. 33A-4-016.** TIH<sub>2</sub>PO<sub>4</sub> (TDP).  $v$  vs.  $T$  [91Han].  $v$ : transverse acoustic wave velocity with wave vector  $\mathbf{q} \parallel [100]$  and polarization vector  $\boldsymbol{\xi} \parallel [001]$ .  $f = 10$  MHz. Dashed curves are smooth extension of  $v$ – $T$  relation to  $\mathcal{O}_{\text{II-I}}$ .



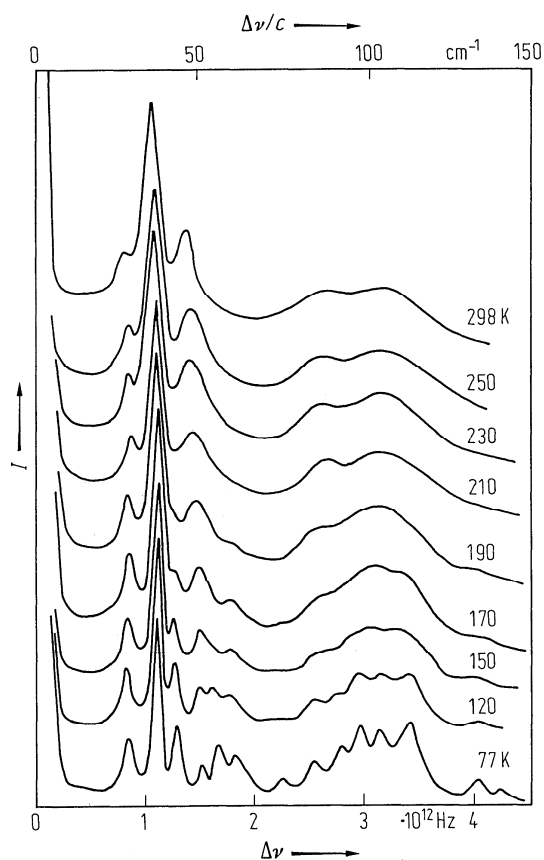


**Fig. 33A-4-017.**  $\text{TiH}_2\text{PO}_4$  (TDP).  $I$  vs.  $\Delta\nu$  [76Huo]. Parameter:  $T$ .  $I$ : Raman scattering intensity of a non-oriented single crystal.

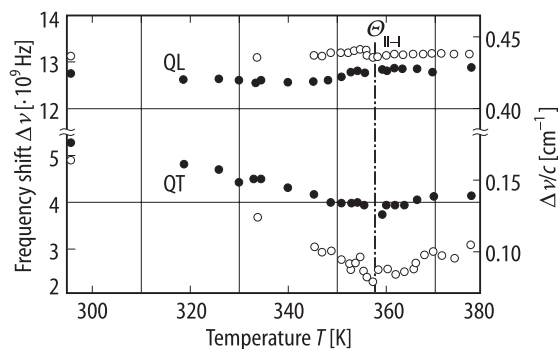


**Fig. 33A-4-018.**  $\text{TiH}_2\text{PO}_4$  (TDP).  $\Delta\nu$  vs.  $T$  [90Ara].  $\Delta\nu$ : Brillouin scattering frequency shift of quasi-longitudinal (QL) and quasi-transverse (QT) modes along the direction of  $\theta = 8^\circ$  (full circle) and  $\theta = 18^\circ$  (open circle) in the  $ac$  plane.

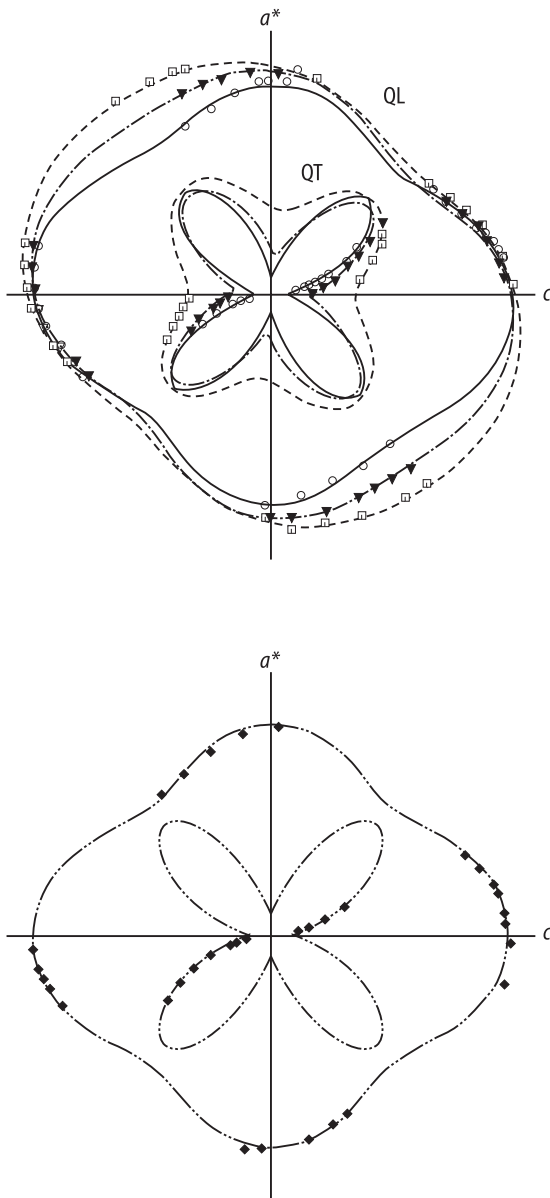


**Fig. 33A-4-019.**  $\text{TlH}_2\text{PO}_4$  (TDP). Angular dependence of  $(\Delta\nu)^2$  in the  $a^*c$  plane [90Ara]. Parameter:  $T$ .  $\Delta\nu$ : Brillouin scattering frequency shift. Open square: 295.6 K, full triangle: 333.6 K, open circle: 335.7 K, full diamond: 359.1 K. QL: quasi-longitudinal mode, QT: quasi-transverse mode.

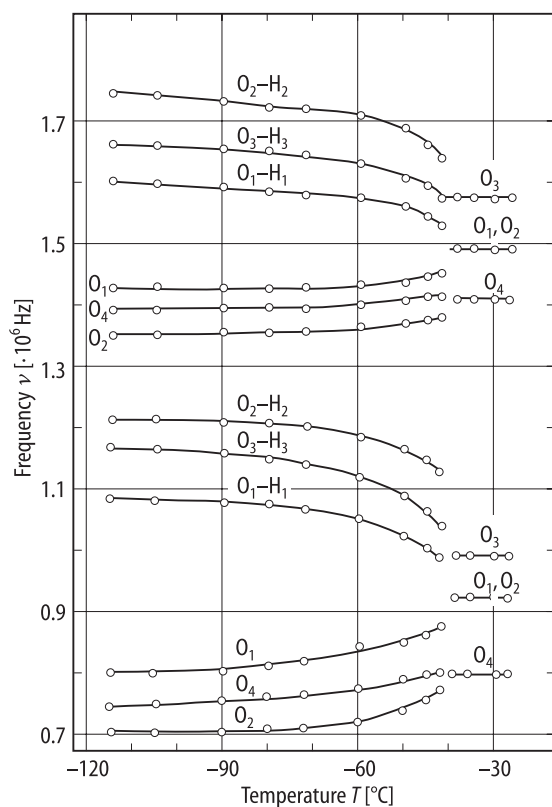


**Fig. 33A-4-020.**  $\text{TiH}_2\text{PO}_4$  (TDP).  $\nu$  vs.  $T$  [88Sel].  $\nu$ :  $^{17}\text{O}$  NQR frequency.  $\nu$  of O atoms with short O–H distance in the hydrogen bond are denoted as  $\text{O}_i\text{--H}_i$  ( $i = 1, 2, 3$ ).

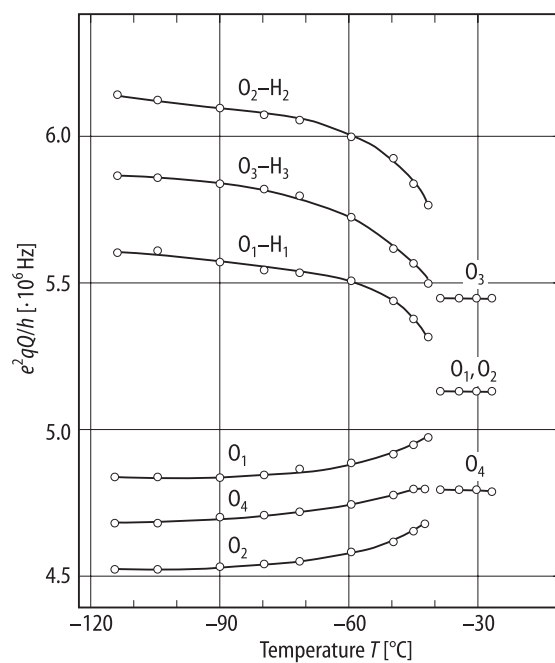


**Fig. 33A-4-021.**  $\text{TiH}_2\text{PO}_4$  (TDP).  $e^2qQ/h$  vs.  $T$  of  $^{17}\text{O}$  [88Sel].  $e^2qQ/h$  of O atoms with short O–H distances in the hydrogen bond are denoted as  $\text{O}_i\text{--H}_i$  ( $i = 1, 2, 3$ ).

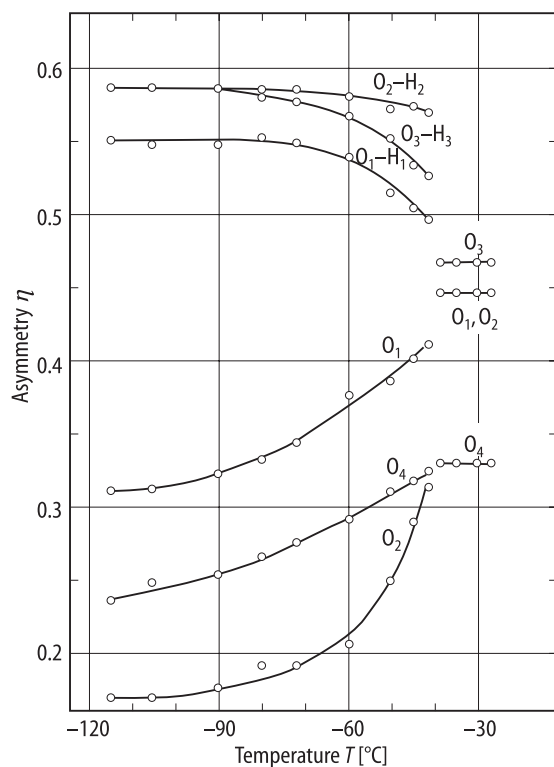


**Fig. 33A-4-022.**  $\text{TiH}_2\text{PO}_4$  (TDP).  $\eta$  vs.  $T$  [88Sel].  $\eta$ : asymmetry parameter of  $^{17}\text{O}$ .  $\eta$  of O atoms with short O–H distances in the hydrogen bond are denoted as  $\text{O}_i\text{–H}_i$  ( $i = 1, 2, 3$ ).

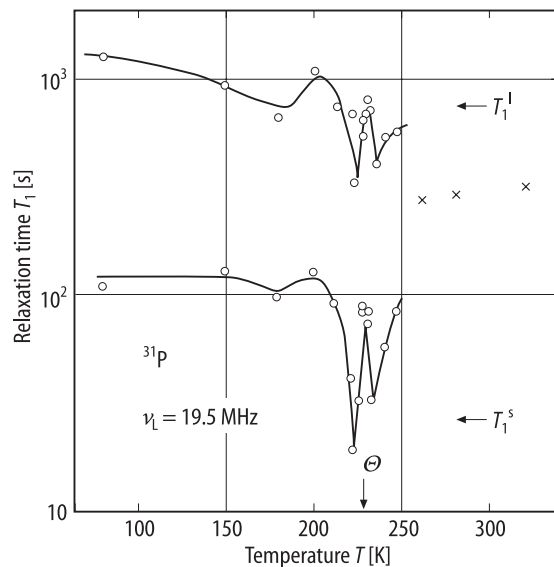


**Fig. 33A-4-023.**  $\text{TiH}_2\text{PO}_4$  (TDP).  $T_1$  vs.  $T$  [88Nak].  $T_1$ :  $^{31}\text{P}$  spin lattice relaxation time. Superscripts l and s denote the long and short components, respectively.

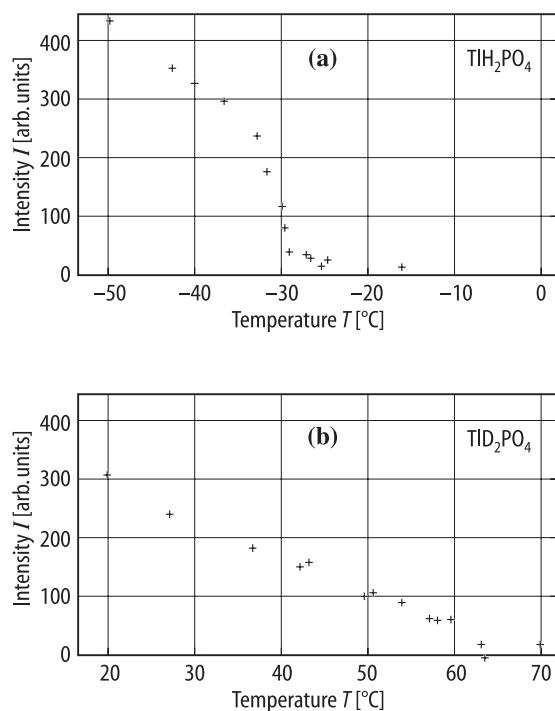


**Fig. 33A-4-024.**  $\text{TIH}_2\text{PO}_4$  (TDP),  $\text{TID}_2\text{PO}_4$  (DTDP).  $I$  vs.  $T$  [81Nel1].  $I$ : X-ray integrated intensity of superlattice reflection at (8.5, 1.5, 1). (a)  $\text{TIH}_2\text{PO}_4$ , (b)  $\text{TID}_2\text{PO}_4$  (deuteration rate > 0.9). New superlattice reflections appear below 230 K in (a) and below 350 K in (b).